TABLE 3. Distribution of Wfs1 Immunoreactivity in the Normal Mouse Optic Nerve

Optic Nerve Cells	
Astrocytes	–
Oligodendrocytes	–
Microglia	–

+, present; –, not present.

9E,F). Extremely weak or no immunoreactivity was seen in the optic chiasm, the optic tract, the LGN, the pretectum, and in the medial terminal nucleus (Fig. 10C,D; Table 4). When a normal rabbit immunoglobulin was used instead of the anti-Wfs1 antibody, no immunoreactivity was seen in the visual cortex, the SCN, and in the SC (data not shown). When the antibody preabsorbed by incubation with the GST-Wfs1N chimeric protein (antigen), immunoreactivity was not observed in these structures (Fig. 10B, data not shown).

DISCUSSION

We determined the expression pattern of the *Wfs1* gene in the normal mouse retina, optic nerve, SC, SCN, and in the visual cortex, at both the mRNA and protein levels. In these structures, not only neurons but also glial cells expressed Wfs1. In the retina, Wfs1 was expressed in all neuron types: photoreceptors, horizontal cells, bipolar cells, displaced (ON) and nondisplaced (OFF) amacrine cells, and RGCs. Müller glial cells also expressed Wfs1. In the optic nerve astrocytes were the site of Wfs1 expression. In the brain, Wfs1 was expressed in the zonal, superficial gray, and intermediate gray layers of the SC, in the dorsomedial part of the SCN, and in layer II of the primary and secondary visual cortical areas.

Specificity of anti-Wfs1 antibody

In the immunoblot analysis, the anti-Wfs1 antibody clearly recognized a single ≈100 kDa protein band of extracts from the brain and optic nerve (Fig. 1). The band size was consistent with an apparent molecular mass of ≈100 kDa that was examined in extracts from rodent brains (Takeda et al., 2001; Ishihara et al., 2004). This protein band disappeared when the antibody was preincubated with the antigen (GST-Wfs1N chimeric protein) (antibody-absorption experiment) (Fig. 1). Thus, the specificity of the antibody has been characterized in the mouse optic nerve as well as in the brain.

Fig. 8. Cellular localization of Wfs1 in the normal mouse optic nerve. **A–I:** Double immunostaining for Wfs1 (Wfs1; A,D,G; Alexa Fluor 488 label; green) and for an astrocyte marker (glial fibrillary acidic protein, GFAP; B,E,H; Alexa Fluor 594 label; red). Cell nuclei are labeled in blue with bisBenzimide (Hoechst 33258). C,F,I are overlaid images. Arrows and arrowheads in A–C indicate the border between intraretinal (i) and astrocytic filament dense (afd) parts, and the boundary between the afd and astrocytic filament sparse (afs) parts, respectively. D–F,G–I are higher-magnification photomicrographs of the afd and afs parts, respectively. These panels show that Wfs1 immunoreactivity is observed in astrocytes. **J–O:** Double immunostaining for Wfs1 (Wfs1; J,M; Alexa Fluor 488 label; green) and for an oligodendrocyte marker (RIP; K,N; Alexa Fluor 594 label; red). Cell nuclei are labeled in blue with bisBenzimide (Hoechst 33258). L,O are overlaid images. M–O are higher-magnification photomicrographs of the afs part. These panels show that Wfs1 immunoreactivity is not seen in oligodendrocytes. **P–R:** Double immunostaining for Wfs1 (Wfs1; P; Alexa Fluor 488 label; green) and for a glial cell marker (glutamine synthetase, GS; Q; Alexa Fluor 594 label; red). R is an overlaid image. Arrows and arrowheads indicate the border between i and afd parts, and the boundary between the afd and afs parts, respectively. Insets are higher-magnification photomicrographs around the boundary between the afd and afs parts. These panels and insets show that colocalization of Wfs1 immunoreactivity and GS immunoreactivity is not seen in the optic nerve but in the retina. These fluorescence photomicrographs were taken with FV500 (Olympus; A–O), and with LSM 510 (Carl Zeiss; P–R) confocal microscopes. Scale bars = 100 μm in C applies to A,B, J–L; 20 μm in O applies to D–I, M,N; 200 μm in R applies to P–Q; 20 μm in inset of R applies to insets of P–Q.

In the immunoblot analysis of retinal extracts the antibody detected both ≈100 kDa and ≈70 kDa bands. As for the ≈70 kDa Wfs1-immunoreactive band, a few reports have appeared. It is not known which kind of protein around ≈70 kDa the antibody detected. If the protein of this band is a part of the Wfs1 protein the appearance of the band likely resulted from degradation of the Wfs1 protein or from an alternative RNA splicing of the *Wfs1* gene in retinal cells. Since not only the ≈100 kDa band but also the ≈70 kDa band disappeared in the antibody-absorption experiment, the protein of ≈70 kDa is most probably a part of the Wfs1 protein containing a portion of the N-terminus antigen site (amino acids 1–179), that is, the antibody can be regarded as Wfs1-specific in the retina. However, there is a remote possibility that the anti-Wfs1 antibody detected a protein at ≈70 kDa other than Wfs1. This possibility will be verified by the immunoblot analysis of retinal extracts from *Wfs1* knockout mice, and by in situ hybridization histochemistry in retinal sections of the normal mouse.

Differences in localization of *Wfs1* expression between the mRNA and protein

There are clear differences in the localization of *Wfs1* expression between the mRNA and protein. In the retina, *Wfs1* mRNA was expressed in the ONL, INL, and GCL where cell bodies are concentrated, while Wfs1 protein was expressed not only in the ONL, INL, and GCL, but also in the OPL and IPL, where processes of retinal cells are accumulated (Fig. 2). Similar differences were also observed in the CA1 field of the hippocampus. In this region, *Wfs1* mRNA expression was confined to the pyramidal cell layer where cell bodies of pyramidal neurons are located, while Wfs1 protein was present not only in the pyramidal cell layer but also in the three strata (strata radiatum, lacunosum-moleculare, and oriens) where processes of pyramidal neurons are extended (Fig. 9A–C). Since the specificity of the anti-Wfs1 antibody in the CA1 field was strictly verified by the immunoblot analysis (present study) and by using *Wfs1* knockout mice (Ishihara et al., 2004), it is reasonable to speculate that the differences are not attributable to a nonspecific immunoreaction of the antibody, but to divergence in the localization of *Wfs1* expression between the mRNA and protein. In the retina, Wfs1 was expressed in all neuron types (photoreceptors, horizontal cells, bipolar cells, nondisplaced and displaced amacrine cells, and RGCs), and in Müller cells. Cell bodies of these cells are confined to the ONL, INL, and to GCL, and *Wfs1* mRNA expression was also confined to these layers. Therefore, there is little discrepancy in the localization of *Wfs1* expression between the mRNA and protein.

In addition, a neurobiological study reported that Wfs1 protein in the brain is found at higher steady-state levels than expected from the relatively low amount of *Wfs1* mRNA (Hofmann et al., 2003). Based on this evi-

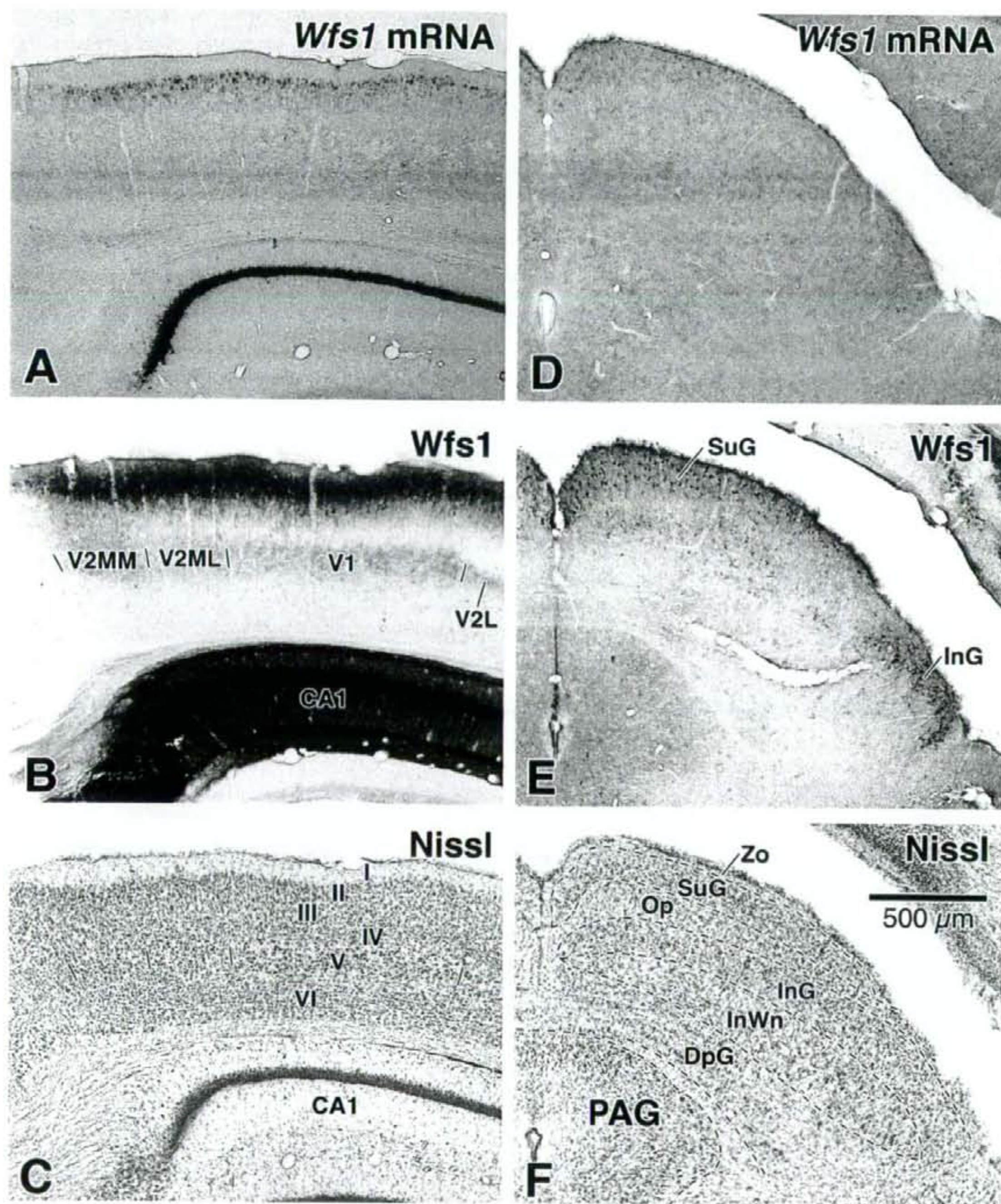

Fig. 9. *Wfs1* mRNA signals and protein immunoreactivity in the normal mouse brain. **A–C:** Mouse *Wfs1* mRNA signals (*Wfs1* mRNA; A), mouse Wfs1 protein immunoreactivity (Wfs1; B), and cytoarchitecture (Nissl; C) in three serial sections of the visual cortex hybridized with antisense cRNA probes of the mouse *Wfs1* 5′-terminus, immunostained with rabbit antimouse Wfs1 N-terminus antibody, and Nissl-stained with cresyl violet, respectively. Short lines in B,C indicate borders between each cortical area. These panels show that both *Wfs1* mRNA signals and Wfs1 immunoreactivity are observed in layer II of the visual cortex. V1, primary visual cortex; V2L, lateral area of the secondary visual cortex; V2ML, mediolateral area of the secondary visual cortex; V2MM, mediomedial area of the secondary visual cortex; CA1, CA1 field of the hippocampus; I, layer I; II, layer II; III, layer III; IV, layer IV; V, layer V; VI, layer VI. **D–F:** Mouse *Wfs1* mRNA signals (*Wfs1* mRNA; D), mouse Wfs1 protein immunoreactivity (Wfs1; E), and cytoarchitecture (Nissl; F) in three serial sections of the superior colliculus (SC). Dashed lines in F indicate borders of each superior collicular layer and the boundary of the periaqueductal gray (PAG). These panels show that *Wfs1* mRNA signals and Wfs1 immunoreactivity are seen in the zonal (Zo), superficial gray (SuG), and intermediate gray (InG) layers of the SC. Op, optic nerve layer of the SC; InWh, intermediate white layer of the SC; DpG, deep gray layer of the SC. Scale bar = 500 μm in F applies to A–E.

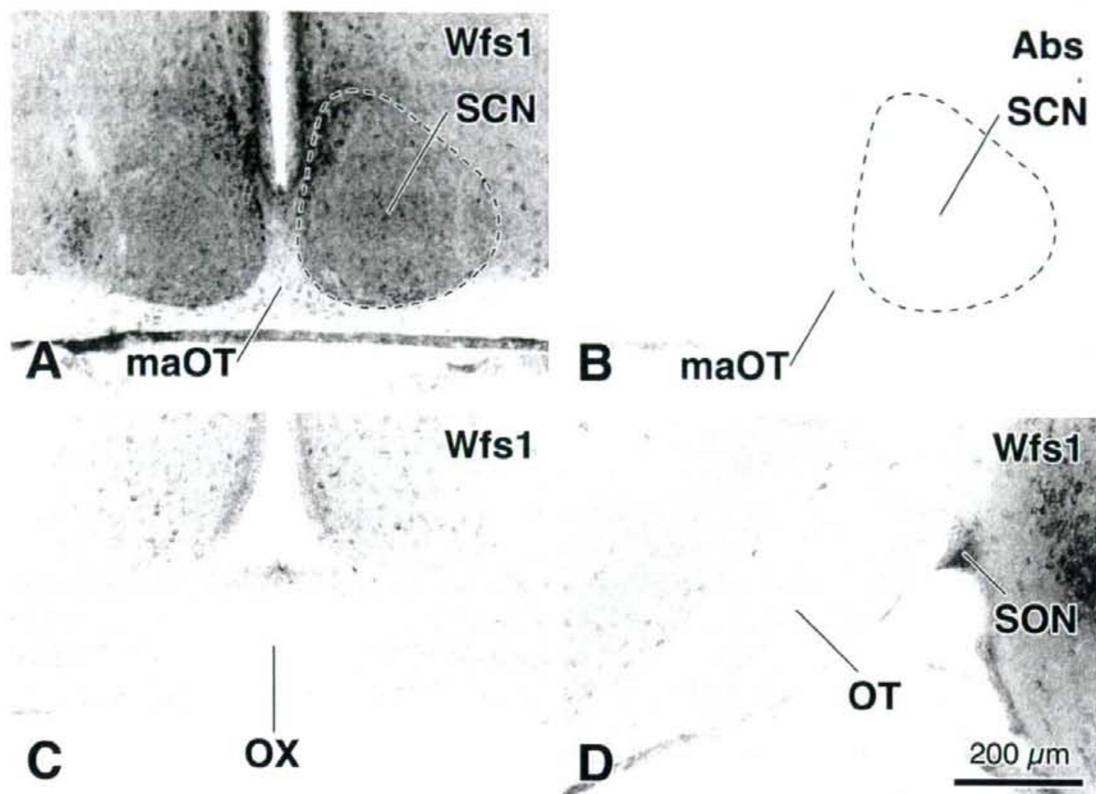

Fig. 10. Wfs1 protein immunoreactivity in the normal mouse suprachiasmatic nucleus (SCN), optic chiasm (OX), and optic tract (OT). **A,B:** Mouse Wfs1 protein immunoreactivity in two adjacent sections of the SCN immunostained with rabbit anti-Wfs1 N-terminus antibody (Wfs1; A), and with the antibody preabsorbed by incubation with GST-Wfs1 N-terminus chimeric protein (antigen) (Abs; B). The dashed lines indicate the boundary of the SCN. These panels show that moderate Wfs1 immunoreactivity is seen in the SCN. maOT, medial accessory optic tract. **C,D:** Mouse Wfs1 protein immunoreactivity in the OX (C) and OT (D). These panels show that Wfs1 immunoreactivity is not seen in the OX or OT. SON, supraoptic nucleus. Scale bar = 200 μm in D applies to A–C.

TABLE 4. Distribution of Wfs1 Immunoreactivity in the Normal Mouse Vision-Related Brain Structures

Vision-Related Brain Structures	
Optic chiasm	–
Optic tract	–
Suprachiasmatic nucleus	+
Lateral geniculate nucleus	–
Pretectum	–
Superior colliculus	+
Medial terminal nucleus	–
Primary visual cortex	+
Secondary visual cortex	+

+, present; –, not present.

dence it is reasonable to accept that the *Wfs1* mRNA expression is weaker than the protein expression in the retina. Therefore, results obtained achieve a reconciliation between *Wfs1* mRNA and protein expression in the retina.

Comparison with previous findings

Yamamoto et al. (2006) showed strong WFS1 immunolabeling in RGCs and optic nerve glial cells of the cynomolgus monkey. In the mouse, Wfs1 was expressed not only in RGCs but also in photoreceptors, horizontal cells, bipolar cells, amacrine cells, and in Müller cells of the retina. In the optic nerve, Wfs1 was present solely in astrocytes. In the brain, Takeda et al. (2001) described Wfs1 expression in layer II of the rat visual cortex. In the mouse, Wfs1 was expressed in the SC and SCN as well as in layer II of the visual cortex. These findings indicate that Wfs1 expression in RGCs, optic nerve glial cells, and in layer II of the visual cortex is similar among various mammalian species.

Retina

Photoreceptors. As for *Wfs1* mRNA expression in the inner segment, verification is necessary, since the inner segment is not a common site of mRNA accumulation. Results obtained clearly showed that *Wfs1* mRNA signals detected by antisense probes were much stronger than

those detected by sense probes (Fig. 2A,B). In addition, several histochemical studies have reported the distribution of mRNA signals in the inner segment (Bumsted et al., 1997; Cowlen et al., 2003; Nogami et al., 2006; Acar et al., 2007). Thus, it is reasonable to speculate that *Wfs1* mRNA is present in the inner segment.

Wfs1 protein immunoreactivity was observed in a majority of cell bodies in the ONL (Fig. 2C). Since rods make up 97.2% and cones 2.8% of all the photoreceptors in the C57 mouse retina (Jeon et al., 1998), the results obtained suggest that Wfs1 is expressed at least in rods. We also demonstrated that both *Wfs1* mRNA and protein were expressed in the inner segments and cell bodies of photoreceptors. Since Wfs1 was not expressed in the outer segments, it is possible that Wfs1 is not directly involved in phototransduction proper in this segment. Instead, Wfs1 is probably distributed as an ER membrane protein in the inner segments and cell bodies of photoreceptors (Takeda et al., 2001; Hofmann et al., 2003), and is considered responsible for the maintenance of phototransduction. In addition, slight photoreceptor dysfunction is suspected in Wolfram syndrome patients (Yamamoto et al., 2006), since the subjective dark adaptation curve in Wolfram syndrome patients shows a diminution of both cone and rod adaptation (Mtanda et al., 1986).

Horizontal cells. Since Wfs1-immunoreactive horizontal cells were calbindin-D-28K positive, Wfs1 was expressed at least in the axon-bearing type (Haverkamp and Wässle, 2000). This evidence indicates for the first time a possible role for this cell type in the pathologic course of Wolfram syndrome. In Wolfram syndrome patients low visual acuity and color visual disturbance are observed (Mtanda et al., 1986; Bitoun, 1994; Seynaeve et al., 1994; Barrett et al., 1997). According to a review by Wässle (2004), horizontal cell dendrites are inserted as lateral elements into the invaginating contacts of cone pedicles, and horizontal cell axon terminals form the lateral elements within rod spherules. Traditionally, it is assumed that horizontal cells release the inhibitory transmitter GABA (γ-aminobutyric acid) and provide feedback inhibition at the photoreceptor synaptic terminal. As horizontal cells summate light signals from several cones, such feedback would cause lateral inhibition, through which a cone's light response is reduced by the illumination of neighboring cones. This mechanism is thought to enhance the response to the edges of visual stimuli and to reduce the response to areas of uniform brightness (Wässle, 2004). Horizontal cell feedback in fish and turtle retinae seems to be cone-specific. However, no such chromatic organization of horizontal cell feedback has been observed in the primate retina, including the human retina (Dacey et al., 1996; Wässle, 2004). Thus, dysfunction of WFS1 protein in horizontal cells might be involved in the low visual acuity in Wolfram syndrome patients rather than color visual disturbance.

Bipolar cells. The Wfs1 immunoreactivity in rod and ON-cone bipolar cells is reliable for the following reasons. Wfs1/Goα double-labeled cells were observed in both the intermediate row of the INL (where cone bipolar cells are distributed) and in the outer row of the INL (where rod bipolar cells are located) (Haverkamp and Wässle, 2000). The immunoreactivity was verified by absorption experiments (Fig. 3G–I). Finally, certainty of the immunoreactivity was also supported by the weak *Wfs1* mRNA signals in the outer and intermediate rows of the INL (Fig. 2A,B).

Wfs1 immunoreactivity in OFF-cone bipolar cells was not examined in the present study. Markers for OFF-cone bipolar cells offered by Haverkamp and Wässle (2000) are Pep19, recoverin, glutamate transporter 1 (GLT-1), and caldendrin. In their study, all antibodies against these marker proteins were generated by a rabbit (Haverkamp and Wässle, 2000). Unfortunately, the anti-Wfs1 antibody was also generated by a rabbit, and the antibody produced perikaryon staining as the antibodies against the marker proteins did (Haverkamp and Wässle, 2000). To examine Wfs1 expression in the OFF-cone bipolar cells it is necessary to obtain other OFF-cone bipolar cell-specific antibodies generated by an animal other than the rabbit.

Amacrine cells. Strong Wfs1 expression was present in cholinergic amacrine cells (Figs. 3J–K, 4A–F). These cholinergic amacrine cells are starburst amacrine cells (Jeon et al., 1998), occurring as matching pairs of displaced (ON) and nondisplaced (OFF) amacrine cells, and their dendrites form two narrow strata in the IPL (Fig. 3K; Haverkamp and Wässle, 2000). It is known that cholinergic amacrine cells are a key element of the direction-selective circuitry. It is likely that both presynaptic and postsynaptic mechanisms are involved in the generation of direction-selective light responses (Yoshida et al., 2001; Euler et al., 2002; Fried et al., 2002; Taylor and Vaney, 2002, 2003; Wässle, 2004). Thus, dysfunction of WFS1 protein in cholinergic amacrine cells might contribute to the disturbance of direction-selective light responses in Wolfram syndrome patients.

RGCs (retinal ganglion cells). Since RGCs make up only 41% of all the neurons in the GCL of the C57 mouse retina (Jeon et al., 1998), we carefully examined Wfs1 expression in RGCs by Wfs1/tracer double labeling and by Wfs1/retinal ganglion cell-specific-marker double immunohistochemistry. Wfs1 expression in RGCs is reliable for the following reasons. Wfs1 expression was detected in RGCs retrogradely labeled with Fluorescent Latex Microspheres (Fig. 4G–I) or with Fluoro-Ruby (Fig. 5A–C), and the expression was verified by the control (preabsorption) experiments (Fig. 4J–L). Wfs1 expression was detected in RGCs immunolabeled with retinal ganglion cell markers: tubulin, βIII isoform, and Brn-3a (Fig. 4M–R). Noncholinergic but Wfs1-immunoreactive cells were distributed in the GCL (Fig. 4A–F). Probably most of these cells are Wfs1-immunoreactive ganglion cells, since the majority of displaced amacrine cells are cholinergic (Voigt, 1986; Brecha et al., 1988; Haverkamp and Wässle, 2000). Finally, the majority of calbindin-D-28K immunolabeled cells in the GCL were double-labeled with Wfs1 (Fig. 3M–O). A proportion of these Wfs1/calbindin-D-28K double-labeled cells are RGCs, since calbindin-D-28K is a marker for both RGCs and displaced amacrine cells in the GCL (Haverkamp and Wässle, 2000). Thus, Wfs1 is present in RGCs as well as in displaced amacrine cells in the GCL.

It is not well known which types of RGCs express Wfs1. Figure 4P–R shows that Wfs1 immunoreactivity is detected in both strongly and weakly Brn-3a-immunolabeled ganglion cells. Since Brn-3a is expressed at high levels in small ganglion cells but not in large ganglion cells, it is possible that Wfs1 is expressed in both small and large ganglion cells (Xiang et al., 1995; Haverkamp and Wässle, 2000).

IPL (inner plexiform layer). The mouse IPL is subdivided into five sublayers of equal thickness. These sublayers can be easily defined by immunolabeling the retina

for the calcium-binding proteins calbindin and calretinin, which shows three strongly labeled horizontal strata of processes (Fig. 3N; Haverkamp and Wässle, 2000; Wässle, 2004). Since the three Wfs1-immunoreactive strata in the IPL corresponded to those immunoreactive for the calcium-binding proteins (Fig. 3M–O), Wfs1 can be used as a marker for the three strongly labeled horizontal strata. In addition, the three strata contain Wfs1-immunoreactive processes of calbindin-D-28K-labeled amacrine and ganglion cells (Fig. 3M–O), since calbindin-D-28K is a marker for both amacrine and ganglion cells (Haverkamp and Wässle, 2000). Of these strata, the inner and outer strata also contain Wfs1-immunoreactive processes of cholinergic amacrine cells, since the two strata were immunoreactive for ChAT (Fig. 3J–L; Haverkamp and Wässle, 2000).

According to a review by Wässle (2004), the outer stratum contains the processes of the OFF-cholinergic amacrine cells, the dendrites of OFF-alpha cells, and the outer dendritic branches of direction selective cells. This band is densely packed with synapses and $GABA_A$ receptors (Brandstätter et al., 1995), and is where transient light responses and OFF direction-selective responses are calculated (Roska and Werblin, 2001). The intermediate stratum separates the OFF sublamina (outer) from the ON sublamina (inner). The polyaxonal amacrine cells (Ölveczky et al., 2003) ramify in this band, as do two GABA-containing amacrine cells. These cells contain, as well as GABA, a neuromodulator (nitric oxide and a catecholamine, respectively). Their functions are unknown. The inner stratum contains the axon terminals of an ON bipolar cell (Brown and Masland, 1999), the processes of the ON-cholinergic amacrine cells, the dendrites of ON-alpha cells, and the inner dendritic branches of direction-selective cells. This stratum is also densely packed with synapses and $GABA_A$ receptors, providing the circuitry for ON-transient light responses and ON direction-selective responses (Wässle, 2004). Thus, it is speculated that the inner stratum contains Wfs1-immunoreactive processes of bipolar cells, as well as those of amacrine and ganglion cells.

Müller cells. Wfs1 protein was expressed strongly in endfeet of Müller cells, moderately in internal radial processes, and weakly in cell bodies, whereas *Wfs1* mRNA signals were weak in the middle row of the INL where cell bodies of Müller cells are located. These results suggest that the turnover of Wfs1 protein in Müller cells is slower than that in other Wfs1-positive retinal neurons. As described above, Wfs1 protein was distributed densely in the endfeet of Müller cells, but sparsely in cell bodies. This evidence indicates that Wfs1 protein accumulates in the endfeet of Müller cells. Elucidating the cause of this accumulation might provide a clue as to the biochemical function of Wfs1 in glial cells including Müller cells.

Although Wolfram syndrome patients often develop diabetes mellitus early on (median age 6 years, range 3 weeks to 16 years; Barrett et al., 1997), they rarely develop diabetic retinopathy (Mtanda et al., 1986; Bitoun, 1994; Seynaeve et al., 1994; Barrett et al., 1997). Diabetic retinopathy is accompanied by a proliferation of new retinal vessels under hypoxic conditions. The proliferation is mediated by Müller cells via the release of vascular endothelial growth factor (VEGF) and transforming growth factor β or via direct contact with endothelial cells (Bringmann and Reichenbach, 2001). In Wolfram syndrome patients it is suggested that the functions of Müller cells are disrupted by loss-of-function mutations in the *WFS1* gene. Thus, the proliferation of new retinal vessels might be hampered by dysfunctional Müller cells in Wolfram syndrome patients.

Optic nerve

Mice lack intraretinal myelination and a well-developed lamina cribrosa but exhibit a marked concentration of astrocytic filaments at the retinal optic nerve junction (Morcos and Chan-Ling, 2000). Based on this evidence, we divided the mouse optic nerve into three parts (i, afd, and afs) defined by the position of the sensory retina and by the distribution of astrocytic filaments. These criteria for the optic nerve subdivisions are appropriate since the distribution of GS-positive cells corresponded to the afs part. Thus, mouse optic nerve is also divided into three parts by the position of the sensory retina and by the distribution of GS-positive cells as shown in Figure 8Q.

Wfs1-positive astrocytes were distributed in the optic nerve, but not in the retina, optic chiasm, or optic tract (Figs. 8A–I, 10C,D). This evidence suggests that the astrocytes in the optic nerve are different from those in the retina, optic chiasm, and optic tract. Further studies are required to clarify the morphological and functional differences between Wfs1-positive astrocytes in the optic nerve and Wfs1-negative astrocytes in the optic chiasm and the optic tract. These studies could provide valuable insights into the physiological role of Wfs1 protein in astrocytes.

Vision-related brain structures

Superior colliculus. The superficial gray layer receives visual inputs directly from the retina and occipital cortex and contains cells that project extrinsically to dorsal thalamic nuclei (Edwards et al., 1986), whereas the intermediate gray layer receives indirect retinal inputs by way of the lateral division of the ventral lateral geniculate nucleus (Brauer and Schober, 1982). Wfs1-positive neurons in the intermediate gray layer as well as those in the superficial gray layer might be involved in visual functions. Neuropathological studies have demonstrated neuronal loss and gliosis in the SC of Wolfram syndrome patients (Genís et al., 1997; Shannon et al., 1999). These findings might be attributed to dysfunctional SC neurons in Wolfram syndrome patients due to loss-of-function mutations in the *WFS1* gene.

Suprachiasmatic nucleus. The SCN is a circadian pacemaker. In the SCN, Wfs1-positive neurons were distributed in the dorsomedial region. This region does not receive direct retinal inputs, but does receive inputs from nonvisual sources. The region sends large numbers of axons to the hypothalamus and small numbers of axons to the thalamus, including the paraventricular thalamic nucleus (PVT). In the PVT, circadian timing information from the SCN is conveyed to multiple limbic structures including the amygdala and the limbic cortical areas (Watts and Swanson, 1987; Kawano et al., 2001; Leak and Moore, 2001). Thus, it is speculated that Wfs1-positive neurons in the dorsomedial part of the SCN provide circadian timing cues to the hypothalamus, the thalamus, and even to the multiple limbic structures without receiving direct retinal inputs.

Visual cortex. The laminar distribution of Wfs1-positive neurons in layer II was present throughout the

mouse neocortex (Kawano et al., unpubl. obs.), as described in the rat (Takeda et al., 2001). Therefore, the distribution is not restricted to the visual cortex. Few thalamic afferents to the visual cortex terminate in layer II (afferents to V1 principally arise in the dorsal lateral geniculate nucleus; Peters and Feldman, 1976; afferents to V2 mainly arise in the lateral posterior nucleus; Olavarria, 1979), but associational afferents from other visual cortical areas terminate in layer II (Coogan and Burkhalter, 1990, 1993). Layer II neurons send associational fibers to the other visual cortical areas (Miller and Vogt, 1984a; Sanderson et al., 1991). Apart from the associational connections, the commissural neurons and terminals are concentrated in a narrow region (the border between V1 and V2L) where the vertical meridian is represented (Cipolloni and Peters, 1979; Cusick and Lund, 1981). In this region, layer II neurons send commissural fibers to and receive commissural fibers from the opposite cortex (Miller and Vogt, 1984b; Sefton et al., 1991). In addition, local circuit neurons are also located in layer II. These neurons make widespread connections within the same layer and project strongly to layer V (Burkhalter, 1989; Sefton and Dreher, 1995). Therefore, Wfs1-immunoreactive punctuations in layer V might be attributed to the strong projections from Wfs1-positive neurons in layer II to layer V. Further studies using tract-tracing methods are required to clarify the fiber connections of Wfs1-positive neurons in layer II. Neuroradiological and neuropathological studies have shown that there is mild cerebrocortical atrophy in Wolfram syndrome patients (Rando et al., 1992; Scolding et al., 1996; Shannon et al., 1999). The atrophy might be attributed to the dysfunctional cortical layer II neurons in Wolfram syndrome patients resulting from loss-of-function mutations in the *WFS1* gene.

Optic atrophy

Optic atrophy is one of the minimal diagnostic criteria for Wolfram syndrome (Barrett et al., 1997). In this section we discuss the pathogenesis of optic atrophy in Wolfram syndrome based on the results obtained. Wfs1 was expressed in all neuron types (RGCs, amacrine cells, bipolar cells, horizontal cells, and photoreceptors) and Müller cells of the retina, in astrocytes of the optic nerve, and in neurons of the SC and the SCN. Out of these cells, candidates for causative cells for optic atrophy in Wolfram syndrome are not only RGCs but also amacrine cells, bipolar cells, SC neurons, SCN neurons, Müller cells, and astrocytes in the optic nerve, since it is speculated that candidate neurons express Wfs1 and are directly connected with RGCs and that cell bodies or axons of RGCs are surrounded by candidate glial cells.

First, we discuss whether RGCs are the principal candidates. In this case, autosomal dominant optic atrophy (ADOA) is useful for comparisons with Wolfram syndrome. ADOA is one of the primary inherited optic neuropathies, and has been attributed to mutations in the *OPA1* gene (Alexander et al., 2000; Delettre et al., 2000; Votruba et al., 2003). OPA1 protein expression is present in RGCs in the mouse, rat, and human (Aijaz et al., 2004; Pesch et al., 2004; Ju et al., 2005). The pattern electroretinogram (PERG) in ADOA patients shows an abnormal N95:P50 ratio, with a reduction in the amplitude of the N95 waveform (Berninger et al., 1991; Holder et al., 1998). Since the PERG N95 component is postulated to be specific for the retinal ganglion cell (Ryan and Arden, 1988), this finding supports a ganglion cell origin for ADOA (Votruba et al., 2003). By contrast, the ERG tests in Wolfram syndrome patients revealed normal or only slightly reduced responses, suggesting that the pathogenesis of the optic atrophy does not lie in the retina, but primarily affects the optic nerve (Niemeyer and Marquardt, 1972; Mtanda et al., 1986; Seynaeve et al., 1994; Barrett et al., 1997). In addition, Barrett et al. (1997) concluded that the reduced visual acuity not due to a refractive error and color vision defect suggested a site of pathology in the visual pathway proximal (posterior) to the eye. Thus, it is possible that the dysfunction of RGCs in Wolfram syndrome patients is mild and that the pathogenesis of optic atrophy is not attributable to the RGCs proper.

Previous clinical, pathological, and neurobiological studies weakly support the notion that amacrine cells, bipolar cells, SC neurons, SCN neurons, and Müller cells are the principal candidates. Although Wfs1 was expressed strongly in amacrine cells and weakly in bipolar cells, there have been few findings of functional abnormality in the INL of Wolfram syndrome patients by using ERGs (Niemeyer and Marquardt, 1972; Mtanda et al., 1986; Seynaeve et al., 1994; Barrett et al., 1997). In the mouse SC, Wfs1-positive cells were distributed in the superficial gray layer where retinal afferents terminate. In Wolfram syndrome patients, neuronal loss and gliosis are observed in the SC (Genís et al., 1997; Shannon et al., 1999). It is possible that optic atrophy is induced by retrograde degeneration of RGCs from the SC. In this case, the degenerated RGCs would be M-cells and K-cells (Y-cells and W-cells in the cat) not P-cells (X-cells in the cat; Garey, 1990; Goebel et al., 2004). By contrast, there is neuronal loss in the LGN mainly involving layers 3–6, which are P-cell relay layers (Garey, 1990; Genís et al., 1997; Goebel et al., 2004) or neuronal loss in all six layers of the LGN (Shannon et al., 1999). If SC neurons are the principal candidates, it is difficult to explain the loss of neurons in the LGN involving the P-cell relay layers. In the mouse SCN, Wfs1-positive neurons are distributed in the dorsomedial part where retinal afferents do not directly terminate. Since strong Wfs1 expression is present in Müller cells, and since RGCs are surrounded by Müller cells, there is a possibility that loss-of-function of Müller cells induces degeneration of RGCs in Wolfram syndrome patients. A neurobiological study using NSE-Hu-Bcl-2 transgenic mice demonstrated that early postnatal Müller cell death leads to retinal degeneration but not optic nerve degeneration (Dubois-Dauphin et al., 2000). It is improbable that Müller cells are the principal candidates. Thus, it is speculated that astrocytes in the optic nerve are the principal candidates for the causative cells for optic atrophy in Wolfram syndrome patients.

Since Wfs1 is expressed in many tissues, the reason why astrocytes in the optic nerve and not other cell types are principally affected by *WFS1* mutations which cause the optic atrophy in Wolfram syndrome is unknown. A biochemical study by using *Xenopus* oocytes suggested that WFS1 protein serves directly as a novel endoplasmic reticulum (ER) calcium channel or, alternatively, as a regulator of ER calcium channel activity. *WFS1* mutations associated with Wolfram syndrome reduce the susceptibility to cation block. It is possible that WFS1 protein-mediated regulation of intracellular calcium provides an important protective function in neurons and/or glial cells that are dependent on the ER for calcium signaling (Hay-

don, 2001; Osman et al., 2003). Recently, a functional study indicated that WFS1 protein expression increases in response to ER stress and that the protein plays a physiological role in protecting cells from ER stress-induced apoptosis (Ueda et al., 2005). Although the biochemical function of WFS1 in neurons and/or glial cells in the visual system remains to be investigated, it is possible that WFS1 mutations in the neurons and/or glial cells cause a disruption of the WFS1-mediated regulation of intracellular calcium levels and/or of the ER stress responses, and a consequent malfunction of electrophysiological activity in the neurons and/or glial cells (Haydon, 2001; Volterra and Meldolesi, 2005; Seifert et al., 2006). This loss-of-function may impair axons of RGCs leading to optic atrophy.

Wfs1 was localized to the afd part of the mouse optic nerve where GS immunoreactivity was almost negative (Figs. 6B, 8Q). This evidence suggests that a lack of GS in the afd part might augment the damage to the optic nerve caused by glutamate. Recently, vesicular glutamate release from axons was demonstrated not only in the corpus callosum but also in the optic nerve of rodents after the propagation of action potentials (Kukley et al., 2007; Ziskin et al., 2007). Thus, impaired glutamate clearance attributable to a lack of GS in the afd part may affect the viability of optic nerve axons in the mouse, including the *Wfs1* knockout mouse.

CONCLUSION

In summary, Wfs1 was present not only in RGCs but also in photoreceptors, horizontal cells, bipolar cells, amacrine cells, and Müller cells of the retina, in astrocytes of the optic nerve, and in neurons of the SC, the SCN, and of the visual cortex. Interestingly, Wfs1 was localized to the afd part of the optic nerve where GS immunoreactivity was almost negative. These results suggest that mutant WFS1 may contribute to the dysfunction of WFS1-expressing neurons and/or glial cells, which may in turn lead to optic atrophy in Wolfram syndrome. They also suggest that the lack of GS in the afd part might augment the damage to the optic nerve caused by glutamate. Although these notions are difficult to test experimentally, the availability of the Wfs1 mouse model could offer opportunities for further investigation. These studies are required to determine the exact physiological role of Wfs1 protein in the biology of vision and to obtain more insights into its pathophysiological roles in optic atrophy in Wolfram syndrome.

ACKNOWLEDGMENTS

The first and corresponding author, June Kawano, thanks Professor Shiro Nakagawa and Associate Professor Satoshi Kuchiiwa (Laboratory for Neuroanatomy, Department of Neurology, Kagoshima University Graduate School of Medical and Dental Sciences) for encouragement and for valuable discussions.

LITERATURE CITED

Acar N, Gregoire S, Andre A, Juaneda P, Joffre C, Bron AM, Creuzot-Garcher CP, Bretillon L. 2007. Plasmalogens in the retina: in situ hybridization of dihydroxyacetone phosphate acyltransferase (DHAP-AT)—the first enzyme involved in their biosynthesis—and comparative study of retinal and retinal pigment epithelial lipid composition. Exp Eye Res 84:143–151.

Aijaz S, Erskine L, Jeffery G, Bhattacharya SS, Votruba M. 2004. Developmental expression profile of the optic atrophy gene product: OPA1 is not localized exclusively in the mammalian retinal ganglion cell layer. Invest Ophthalmol Vis Sci 45:1667–1673.

Alexander C, Votruba M, Pesch UE, Thiselton DL, Mayer S, Moore A, Rodriguez M, Kellner U, Leo-Kottler B, Auburger G, Bhattacharya SS, Wissinger B. 2000. *OPA1*, encoding a dynamin-related GTPase, is mutated in autosomal dominant optic atrophy linked to chromosome 3q28. Nat Genet 26:211–215.

Barrett TG, Bundey SE, Macleod AF. 1995. Neurodegeneration and diabetes: UK nationwide study of Wolfram (DIDMOAD) syndrome. Lancet 346:1458–1463.

Barrett TG, Bundey SE, Fielder AR, Good PA. 1997. Optic atrophy in Wolfram (DIDMOAD) syndrome. Eye 11:882–888.

Berninger TA, Jaeger W, Krastel H. 1991. Electrophysiology and colour perimetry in dominant infantile optic atrophy. Br J Ophthalmol 75:49–52.

Bitoun P. 1994. Wolfram syndrome. A report of four cases and review of the literature. Ophthalmic Genet 15:77–85.

Brandstätter JH, Greferath U, Euler T, Wässle H. 1995. Co-stratification of $GABA_A$ receptors with the directionally selective circuitry of the rat retina. Vis Neurosci 12:345–358.

Brauer K, Schober W. 1982. Identification of geniculo-tectal relay neurons in the rat's ventral lateral geniculate nucleus. Exp Brain Res 45:84–88.

Brecha N, Johnson D, Peichl L, Wässle H. 1988. Cholinergic amacrine cells of the rabbit retina contain glutamate decarboxylase and g-aminobutyrate immunoreactivity. Proc Natl Acad Sci U S A 85:6187–6191.

Bringmann A, Reichenbach A. 2001. Role of Müller cells in retinal degenerations. Front Biosci 6:E72–92.

Brown SP, Masland RH. 1999. Costratification of a population of bipolar cells with the direction-selective circuitry of the rabbit retina. J Comp Neurol 408:97–106.

Bumsted K, Jasoni C, Szél A, Hendrickson A. 1997. Spatial and temporal expression of cone opsins during monkey retinal development. J Comp Neurol 378:117–134.

Burkhalter A. 1989. Intrinsic connections of rat primary visual cortex: laminar organization of axonal projections. J Comp Neurol 279:171–186.

Cipolloni PB, Peters A. 1979. The bilaminar and banded distribution of the callosal terminals in the posterior neocortex of the rat. Brain Res 176:33–47.

Collier DA, Barrett TG, Curtis D, Macleod A, Arranz MJ, Maassen JA, Bundey S. 1996. Linkage of Wolfram syndrome to chromosome 4p16.1 and evidence for heterogeneity. Am J Hum Genet 59:855–863.

Coogan TA, Burkhalter A. 1990. Conserved patterns of cortico-cortical connections define areal hierarchy in rat visual cortex. Exp Brain Res 80:49–53.

Coogan TA, Burkhalter A. 1993. Hierarchical organization of areas in rat visual cortex. J Neurosci 13:3749–3772.

Cowlen MS, Zhang VZ, Warnock L, Moyer CF, Peterson WM, Yerxa BR. 2003. Localization of ocular $P2Y_2$ receptor gene expression by in situ hybridization. Exp Eye Res 77:77–84.

Cryns K, Thys S, Van Laer L, Oka Y, Pfister M, Van Nassauw L, Smith RJ, Timmermans JP, Van Camp G. 2003. The *WFS1* gene, responsible for low frequency sensorineural hearing loss and Wolfram syndrome, is expressed in a variety of inner ear cells. Histochem Cell Biol 119:247–256.

Cusick CG, Lund RD. 1981. The distribution of the callosal projection to the occipital visual cortex in rats and mice. Brain Res 214:239–259.

Dacey DM, Lee BB, Stafford DK, Pokorny J, Smith VC. 1996. Horizontal cells of the primate retina: cone specificity without spectral opponency. Science 271:656–659.

Debus E, Weber K, Osborn M. 1983. Monoclonal antibodies specific for glial fibrillary acidic (GFA) protein and for each of the neurofilament triplet polypeptides. Differentiation 25:193–203.

Delettre C, Lenaers G, Griffoin JM, Gigarel N, Lorenzo C, Belenguer P, Pelloquin L, Grosgeorge J, Turc-Carel C, Perret E, Astarie-Dequeker C, Lasquellec L, Arnaud B, Ducommun B, Kaplan J, Hamel CP. 2000. Nuclear gene *OPA1*, encoding a mitochondrial dynamin-related protein, is mutated in dominant optic atrophy. Nat Genet 26:207–210.

Dráberová E, Lukás Z, Ivanyi D, Viklicky V, Dráber P. 1998. Expression of

class III β-tubulin in normal and neoplastic human tissues. Histochem Cell Biol 109:231–239.

Dräger UC. 1983. Coexistence of neurofilaments and vimentin in a neurone of adult mouse retina. Nature 303:169–172.

Dubois-Dauphin M, Poitry-Yamate C, de Bilbao F, Julliard AK, Jourdan F, Donati G. 2000. Early postnatal Müller cell death leads to retinal but not optic nerve degeneration in NSE-Hu-Bcl-2 transgenic mice. Neuroscience 95:9–21.

Edwards MA, Caviness VS Jr, Schneider GE. 1986. Development of cell and fiber lamination in the mouse superior colliculus. J Comp Neurol 248:395–409.

Euler T, Detwiler PB, Denk W. 2002. Directionally selective calcium signals in dendrites of starburst amacrine cells. Nature 418:845–852.

Fried SI, Munch TA, Werblin FS. 2002. Mechanisms and circuitry underlying directional selectivity in the retina. Nature 420:411–414.

Friedman B, Hockfield S, Black JA, Woodruff KA, Waxman SG. 1989. In situ demonstration of mature oligodendrocytes and their processes: an immunocytochemical study with a new monoclonal antibody, rip. Glia 2:380–390.

Fujinaga R, Kawano J, Matsuzaki Y, Kamei K, Yanai A, Sheng Z, Tanaka M, Nakahama K, Nagano M, Shinoda K. 2004. Neuroanatomical distribution of Huntingtin-associated protein 1-mRNA in the male mouse brain. J Comp Neurol 478:88–109.

Garey LJ. 1990. Visual system. In: Paxinos G, editor. The human nervous system. San Diego: Academic Press. p 945–977.

Gargini C, Terzibasi E, Mazzoni F, Strettoi E. 2007. Retinal organization in the retinal degeneration 10 (rd10) mutant mouse: a morphological and ERG study. J Comp Neurol 500:222–238.

Genis D, Dávalos A, Molins A, Ferrer I. 1997. Wolfram syndrome: a neuropathological study. Acta Neuropathol (Berl) 93:426–429.

Goebel R, Muckli L, Kim DS. 2004. Visual system. In: Paxinos G, Mai JK, editors. The human nervous system. San Diego: Elsevier Academic Press. p 1280–1305.

Gómez-Zaera M, Strom TM, Rodríguez B, Estivill X, Meitinger T, Nunes V. 2001. Presence of a major WFS1 mutation in Spanish Wolfram syndrome pedigrees. Mol Genet Metab 72:72–81.

Hardy C, Khanim F, Torres R, Scott-Brown M, Seller A, Poulton J, Collier D, Kirk J, Polymeropoulos M, Latif F, Barrett T. 1999. Clinical and molecular genetic analysis of 19 Wolfram syndrome kindreds demonstrating a wide spectrum of mutations in WFS1. Am J Hum Genet 65:1279–1290.

Haverkamp S, Wässle H. 2000. Immunocytochemical analysis of the mouse retina. J Comp Neurol 424:1–23.

Haydon PG. 2001. GLIA: listening and talking to the synapse. Nat Rev Neurosci 2:185–193.

Hofmann S, Philbrook C, Gerbitz KD, Bauer MF. 2003. Wolfram syndrome: structural and functional analyses of mutant and wild-type wolframin, the WFS1 gene product. Hum Mol Genet 12:2003–2012.

Holder GE, Votruba M, Carter AC, Bhattacharya SS, Fitzke FW, Moore AT. 1998. Electrophysiological findings in dominant optic atrophy (DOA) linking to the OPA1 locus on chromosome 3q 28-qter. Doc Ophthalmol 95:217–228.

Inoue H, Tanizawa Y, Wasson J, Behn P, Kalidas K, Bernal-Mizrachi E, Mueckler M, Marshall H, Donis-Keller H, Crock P, Rogers D, Mikuni M, Kumashiro H, Higashi K, Sobue G, Oka Y, Permutt MA. 1998. A gene encoding a transmembrane protein is mutated in patients with diabetes mellitus and optic atrophy (Wolfram syndrome). Nat Genet 20:143–148.

Ishihara H, Takeda S, Tamura A, Takahashi R, Yamaguchi S, Takei D, Yamada T, Inoue H, Soga H, Katagiri H, Tanizawa Y, Oka Y. 2004. Disruption of the *WFS1* gene in mice causes progressive β-cell loss and impaired stimulus-secretion coupling in insulin secretion. Hum Mol Genet 13:1159–1170.

Jalil MA, Begum L, Contreras L, Pardo B, Iijima M, Li MX, Ramos M, Marmol P, Horiuchi M, Shimotsu K, Nakagawa S, Okubo A, Sameshima M, Isashiki Y, Del Arco A, Kobayashi K, Satrústegui J, Saheki T. 2005. Reduced *N*-acetylaspartate levels in mice lacking aralar, a brain- and muscle-type mitochondrial aspartate-glutamate carrier. J Biol Chem 280:31333–31339.

Jeon CJ, Strettoi E, Masland RH. 1998. The major cell populations of the mouse retina. J Neurosci 18:8936–8946.

Ju WK, Misaka T, Kushnareva Y, Nakagomi S, Agarwal N, Kubo Y, Lipton SA, Bossy-Wetzel E. 2005. OPA1 expression in the normal rat retina and optic nerve. J Comp Neurol 488:1–10.

Kang TH, Ryu YH, Kim IB, Oh GT, Chun MH. 2004. Comparative study of cholinergic cells in retinas of various mouse strains. Cell Tissue Res 317:109–115.

Kawano J, Krout KE, Loewy AD. 2001. Suprachiasmatic nucleus projections to the paraventricular thalamic nucleus of the rat. Thalamus Relat Syst 1:197–202.

Khanim F, Kirk J, Latif F, Barrett TG. 2001. WFS1/wolframin mutations, Wolfram syndrome, and associated diseases. Hum Mutat 17:357–367.

Kukley M, Capetillo-Zarate E, Dietrich D. 2007. Vesicular glutamate release from axons in white matter. Nat Neurosci 10:311–320.

Leak RK, Moore RY. 2001. Topographic organization of suprachiasmatic nucleus projection neurons. J Comp Neurol 433:312–334.

Miller MW, Vogt BA. 1984a. Direct connections of rat visual cortex with sensory, motor, and association cortices. J Comp Neurol 226:184–202.

Miller MW, Vogt BA. 1984b. Heterotopic and homotopic callosal connections in rat visual cortex. Brain Res 297:75–89.

Minton JA, Rainbow LA, Ricketts C, Barrett TG. 2003. Wolfram syndrome. Rev Endocr Metab Disord 4:53–59.

Morcos Y, Chan-Ling T. 2000. Concentration of astrocytic filaments at the retinal optic nerve junction is coincident with the absence of intra-retinal myelination: comparative and developmental evidence. J Neurocytol 29:665–678.

Mtanda AT, Cruysberg JR, Pinckers AJ. 1986. Optic atrophy in Wolfram syndrome. Ophthalmic Paediatr Genet 7:159–165.

Neufeld AH. 1999. Microglia in the optic nerve head and the region of parapapillary chorioretinal atrophy in glaucoma. Arch Ophthalmol 117:1050–1056.

Niemeyer G, Marquardt JL. 1972. Retinal function in an unique syndrome of optic atrophy, juvenile diabetes mellitus, diabetes insipidus, neurosensory hearing loss, autonomic dysfunction, and hyperalanineuria. Invest Ophthalmol 11:617–624.

Nogami H, Ogasawara K, Minmura Y, Mogi K, Shutoh F, Hisano S. 2006. Developmentally-regulated expression of tissue-specific splice variant of rat vesicular glutamate transporter 1 in retina and pineal gland. J Neurochem 99:142–153.

Olavarria J. 1979. A horseradish peroxidase study of the projections from the latero-posterior nucleus to three lateral peristriate areas in the rat. Brain Res 173:137–141.

Olveczky BP, Baccus SA, Meister M. 2003. Segregation of object and background motion in the retina. Nature 423:401–408.

Osman AA, Saito M, Makepeace C, Permutt MA, Schlesinger P, Mueckler M. 2003. Wolframin expression induces novel ion channel activity in endoplasmic reticulum membranes and increases intracellular calcium. J Biol Chem 278:52755–52762.

Paxinos G, Franklin KBJ. 2001. The mouse brain in stereotaxic coordinates. San Diego: Academic Press.

Pesch UE, Fries JE, Bette S, Kalbacher H, Wissinger B, Alexander C, Kohler K. 2004. *OPA1*, the disease gene for autosomal dominant optic atrophy, is specifically expressed in ganglion cells and intrinsic neurons of the retina. Invest Ophthalmol Vis Sci 45:4217–4225.

Peters A, Feldman ML. 1976. The projection of the lateral geniculate nucleus to area 17 of the rat cerebral cortex. I. General description. J Neurocytol 5:63–84.

Polymeropoulos MH, Swift RG, Swift M. 1994. Linkage of the gene for Wolfram syndrome to markers on the short arm of chromosome 4. Nat Genet 8:95–97.

Rando TA, Horton JC, Layzer RB. 1992. Wolfram syndrome: evidence of a diffuse neurodegenerative disease by magnetic resonance imaging. Neurology 42:1220–1224.

Reichert F, Rotshenker S. 1996. Deficient activation of microglia during optic nerve degeneration. J Neuroimmunol 70:153–161.

Roska B, Werblin F. 2001. Vertical interactions across ten parallel, stacked representations in the mammalian retina. Nature 410:583–587.

Ryan S, Arden GB. 1988. Electrophysiological discrimination between retinal and optic nerve disorders. Doc Ophthalmol 68:247–255.

Saari JC, Huang J, Possin DE, Fariss RN, Leonard J, Garwin GG, Crabb JW, Milam AH. 1997. Cellular retinaldehyde-binding protein is expressed by oligodendrocytes in optic nerve and brain. Glia 21:259–268.

Sanderson KJ, Dreher B, Gayer N. 1991. Prosencephalic connections of striate and extrastriate areas of rat visual cortex. Exp Brain Res 85:324–334.

Scolding NJ, Kellar-Wood HF, Shaw C, Shneerson JM, Antoun N. 1996. Wolfram syndrome: hereditary diabetes mellitus with brainstem and optic atrophy. Ann Neurol 39:352–360.

Sefton AJ, Dreher B. 1995. Visual system. In: Paxinos G, editor. The rat nervous system. San Diego: Academic Press. p 833–898.

Sefton AJ, Dreher B, Lim WL. 1991. Interactions between callosal, thalamic and associational projections to the visual cortex of the developing rat. Exp Brain Res 84:142–158.

Seifert G, Schilling K, Steinhäuser C. 2006. Astrocyte dysfunction in neurological disorders: a molecular perspective. Nat Rev Neurosci 7:194–206.

Seynaeve H, Vermeiren A, Leys A, Dralands L. 1994. Four cases of Wolfram syndrome: ophthalmologic findings and complications. Bull Soc Belge Ophtalmol 252:75–80.

Shannon P, Becker L, Deck J. 1999. Evidence of widespread axonal pathology in Wolfram syndrome. Acta Neuropathol (Berl) 98:304–308.

Sharma RK, Netland PA. 2007. Early born lineage of retinal neurons express class III β-tubulin isotype. Brain Res 1176:11–17.

Sheng Z, Kawano J, Yanai A, Fujinaga R, Tanaka M, Watanabe Y, Shinoda K. 2004. Expression of estrogen receptors (α, β) and androgen receptor in serotonin neurons of the rat and mouse dorsal raphe nuclei; sex and species differences. Neurosci Res 49:185–196.

Strom TM, Hörtnagel K, Hofmann S, Gekeler F, Scharfe C, Rabl W, Gerbitz KD, Meitinger T. 1998. Diabetes insipidus, diabetes mellitus, optic atrophy and deafness (DIDMOAD) caused by mutations in a novel gene (*wolframin*) coding for a predicted transmembrane protein. Hum Mol Genet 7:2021–2028.

Takeda K, Inoue H, Tanizawa Y, Matsuzaki Y, Oba J, Watanabe Y, Shinoda K, Oka Y. 2001. WFS1 (Wolfram syndrome 1) gene product: predominant subcellular localization to endoplasmic reticulum in cultured cells and neuronal expression in rat brain. Hum Mol Genet 10:477–484.

Takei D, Ishihara H, Yamaguchi S, Yamada T, Tamura A, Katagiri H, Maruyama Y, Oka Y. 2006. WFS1 protein modulates the free Ca^{2+} concentration in the endoplasmic reticulum. FEBS Lett 580:5635–5640.

Taylor WR, Vaney DI. 2002. Diverse synaptic mechanisms generate direction selectivity in the rabbit retina. J Neurosci 22:7712–7720.

Taylor WR, Vaney DI. 2003. New directions in retinal research. Trends Neurosci 26:379–385.

Tessa A, Carbone I, Matteoli MC, Bruno C, Patrono C, Patera IP, De Luca F, Lorini R, Santorelli FM. 2001. Identification of novel WFS1 mutations in Italian children with Wolfram syndrome. Hum Mutat 17:348–349.

Ueda K, Kawano J, Takeda K, Yujiri T, Tanabe K, Anno T, Akiyama M, Nozaki J, Yoshinaga T, Koizumi A, Shinoda K, Oka Y, Tanizawa Y. 2005. Endoplasmic reticulum stress induces Wfs1 gene expression in pancreatic β-cells via transcriptional activation. Eur J Endocrinol 153:167–176.

Voigt T. 1986. Cholinergic amacrine cells in the rat retina. J Comp Neurol 248:19–35.

Volterra A, Meldolesi J. 2005. Astrocytes, from brain glue to communication elements: the revolution continues. Nat Rev Neurosci 6:626–640.

von Gräfe A. 1858. Über die mit Diabetes vorkommenden Sehstörungen. Arch Ophthal 4:230–234.

Votruba M, Aijaz S, Moore AT. 2003. A review of primary hereditary optic neuropathies. J Inherit Metab Dis 26:209–227.

Warr WB, de Olmos JS, Heimer L. 1981. Horseradish peroxidase: the basic procedure. In: Heimer L, Robards MJ, editors. Neuroanatomical tract-tracing methods. New York: Plenum Press. p 207–262.

Wässle H. 2004. Parallel processing in the mammalian retina. Nat Rev Neurosci 5:747–757.

Watts AG, Swanson LW. 1987. Efferent projections of the suprachiasmatic nucleus: II. Studies using retrograde transport of fluorescent dyes and simultaneous peptide immunohistochemistry in the rat. J Comp Neurol 258:230–252.

Wolfram DJ, Wagener HP. 1938. Diabetes mellitus and simple optic atrophy among siblings: report of four cases. Mayo Clin Proc 13:715–718.

Xiang M, Zhou L, Macke JP, Yoshioka T, Hendry SH, Eddy RL, Shows TB, Nathans J. 1995. The Brn-3 family of POU-domain factors: primary structure, binding specificity, and expression in subsets of retinal ganglion cells and somatosensory neurons. J Neurosci 15:4762–4785.

Yamaguchi S, Ishihara H, Tamura A, Yamada T, Takahashi R, Takei D, Katagiri H, Oka Y. 2004. Endoplasmic reticulum stress and N-glycosylation modulate expression of WFS1 protein. Biochem Biophys Res Commun 325:250–256.

Yamamoto H, Hofmann S, Hamasaki DI, Kreczmanski P, Schmitz C, Parel JM, Schmidt-Kastner R. 2006. Wolfram syndrome 1 (WFS1) protein expression in retinal ganglion cells and optic nerve glia of the cynomolgus monkey. Exp Eye Res 83:1303–1306.

Yoshida K, Watanabe D, Ishikane H, Tachibana M, Pastan I, Nakanishi S. 2001. A key role of starburst amacrine cells in originating retinal directional selectivity and optokinetic eye movement. Neuron 30:771–780.

Ziskin JL, Nishiyama A, Rubio M, Fukaya M, Bergles DE. 2007. Vesicular release of glutamate from unmyelinated axons in white matter. Nat Neurosci 10:321–330.